ChemComm

Accepted Manuscript

This article can be cited before page numbers have been issued, to do this please use: S. Bartlett, E. Sackville, E. K. Gibson, V. Celorrio, P. P. Wells, M. Nachtegaal, S. W. Sheehan and U. Hintermair, *Chem. Commun.*, 2019, DOI: 10.1039/C9CC02088H.

This is an Accepted Manuscript, which has been through the Royal Society of Chemistry peer review process and has been accepted for publication.

Accepted Manuscripts are published online shortly after acceptance, before technical editing, formatting and proof reading. Using this free service, authors can make their results available to the community, in citable form, before we publish the edited article. We will replace this Accepted Manuscript with the edited and formatted Advance Article as soon as it is available.

You can find more information about Accepted Manuscripts in the author guidelines.

Please note that technical editing may introduce minor changes to the text and/or graphics, which may alter content. The journal's standard Terms & Conditions and the ethical guidelines, outlined in our author and reviewer resource centre, still apply. In no event shall the Royal Society of Chemistry be held responsible for any errors or omissions in this Accepted Manuscript or any consequences arising from the use of any information it contains.

View Article Online
DOI: 10.1039/C9CC02088H

ARTICLE

Evidence for Tetranuclear bis-μ-oxo Cubane Species in Molecular Iridium-based Water Oxidation Catalysts from XAS Analysis

Received 00th January 20xx,
Accepted 00th January 20xx

DOI: 10.1039/x0xx00000x

Stuart A. Bartlett,[b,c]* Emma V. Sackville,[a] Emma K. Gibson,[d,e] Veronica Celorrio,[d] Peter P. Wells,[d,f] Maarten Nachtegaal,[g] Stafford W. Sheehan,[h] and Ulrich Hintermair[a]*

The structure of a highly active pyridine-alkoxide iridium water oxidation catalyst (WOC) is examined by X-ray absorption spectroscopy (XAS). A detailed comparison with IrO_2 points to a rigid molecular unit of low nuclearity, with the best analysis suggesting the existence of a novel tetrameric iridium-oxo cubane as the resting state.

The water oxidation reaction continues to present a major challenge for the efficient transformation of renewable electricity into chemical energy.[1-2] Although a number of well-defined molecular precursors to highly active water oxidation catalysts (WOCs) have been developed,[3-4] there still is a distinct lack of structural and electronic insight into their reaction intermediates. This often hampers the rational development toward improved systems that meet the robustness and stability requirements for practical applications. To date, commercial electrolysers thus exclusively employ heterogeneous metal oxide anodes, with amorphous iridium oxy-hydroxide still standing as the most active and durable WOC material known.[5] A number of recent X-ray absorption spectroscopy (XAS), X-ray photoelectron spectroscopy (XPS), UV-vis spectroscopy, and electrochemistry studies of IrO_x surfaces under working conditions consistently suggest Ir^{III}-Ir^{IV}-Ir^{V} redox cycles across two neighboring metal sites to effect the four-electron oxidation of water to O_2.[6-11]

The geometry of rutile IrO_2 suggests this to be possible through a "diamond core" bis-μ-oxo unit, a structural feature that is also found in many other WOCs based on manganese,[12] ruthenium[13] and cobalt oxides,[14] including the active site of the natural oxygen-evolving complex (OEC) in photosystem II.[15] Over the past decade some highly active molecular Ir-based WOCs have been developed,[16] though some have been shown to rapidly transform into IrO_x nanoparticles *in situ*.[17] Strongly binding and oxidatively robust ligands (such as pyridine-alkoxides[18]) however yield highly active WOC solutions that are fully homogeneous.[19] After activation[20] these can even be grafted onto conducting metal oxides as molecular monolayers to yield exceptionally efficient and durable anodes for electrochemical water oxidation.[21-23] Although a number of spectroscopic features have been analyzed,[24] the exact molecular structure of these highly active catalysts has not yet been elucidated. A previous study of a pyridine-alkoxide ligated Ir WOC using high-energy X-ray scattering (HEXS) analysis and density functional theory (DFT) modelling suggested a mono-μ-oxo Ir dimer as the resting state of the activated catalyst,[25] and in the following a series of coordinately saturated mono-μ-oxo dimers with two pyalk ligands per iridium centre have been synthesised.[26] These intriguing model compounds allowed the direct characterization of higher valent states not observable in the parent catalyst bearing one pyalk ligand per metal, but the question how relevant the mono-μ-oxo motif to catalysis is remains.

Here we present our results from a detailed X-ray absorption spectroscopy study of a molecular Ir-pyalk WOC in solution that provide strong evidence for bis-μ-oxo units in dimeric and tetrameric species as the resting state of the catalyst.

XAS has been successfully employed in several cases to gain structural insight into functional WOCs, including the $CaMn_4$ oxo-cubane OEC in PSII,[27] CoO_x films[14, 28] and molecular Ru WOCs immobilized on surfaces.[29] Here we investigated the activated form of [Cp*Ir(dimethyl-pyridinealkoxide)Cl] obtained by stirring with 50 equivalents of $NaIO_4$ in water at room temperature for 16 hours (termed Ir-pyalk WOC), conditions

[a] Centre for Sustainable Chemical Technologies, University of Bath, Bath BA2 7AY, United Kingdom. E-mail: u.hintermair@bath.ac.uk
[b] Dynamic Structural Science, Rutherford Appleton Laboratory, Research Complex at Harwell OX11 0FA, United Kingdom. E-mail: stuart.bartlett@sydney.edu.au
[c] School of Chemistry, University of Sydney, Sydney NSW 2006, Australia.
[d] Rutherford Appleton Laboratory, UK Catalysis Hub, Research Complex at Harwell OX11 0FA, United Kingdom.
[e] School of Chemistry, University of Glasgow, Glasgow G12 8QQ, United Kingdom.
[f] School of Chemistry, University of Southampton, Southampton SO17 1BJ, United Kingdom.
[g] Paul Scherrer Institute, 5232 Villigen, Switzerland.
[h] Catalytic Innovations LLC, Fall River, MA 02732, United States.
Electronic Supplementary Information (ESI) available: Details of XAS fitting analyses (XANES and EXAFS), structural details and additional plots. See DOI: 10.1039/x0xx00000x

View Article Online
DOI: 10.1039/C9CC02088H

which have previously been shown to yield a homogeneous iridium species without any bound Cp* but retaining the pyalk ligand.[19, 24, 30] XAS measurements were performed directly on freshly prepared 5 mM aqueous solutions, and on cellulose pellets of the dark blue solid obtained after slow evaporation of these solutions to dryness (yielding identical spectra). Reference samples of Ir^0 (metal foil), Ir^I ($[Ir(cod)Cl]_2$), Ir^{III} ($[Cp^*Ir(pyalk)Cl]$ and $[Cp^*Ir(H_2O)_3]SO_4$), and Ir^{IV} ($Na_2[IrCl_6]$ and IrO_2) were measured as standards for the different metal oxidation states. The XAS data was collected at the SuperXAS beamline at the Swiss Light Source and B18 at the Diamond Synchrotron at the iridium L_3 edge at 11 – 12.5 keV in fluorescence mode.

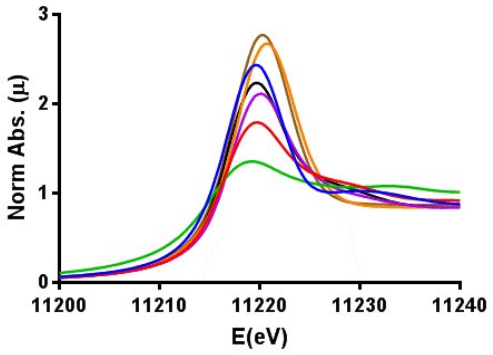

Figure 1. Normalized XANES spectra calibrated to the Pt^0 L_3 edge, displaying iridium L_3 edge energies in Ir^0 foil (green), $[Ir^I(cod)Cl]_2$ (red), $[Cp^*Ir^{III}(H_2O)_3]SO_4$ (purple), $[Cp^*Ir^{III}(pyalk)Cl]$ (black), $Na_2[Ir^{IV}Cl_6]$ (blue), $Ir^{IV}O_2$ (orange), and the Ir-pyalk WOC (brown). For further details see Figure S5.

The comparative XANES of the reference samples (Figure 1) showed a general trend of increasing white line intensity with increasing oxidation states. This is expected due to the Ir L_3 edge X-ray absorption constituting an allowed 2p → 5d transition, where the intensity increases in higher oxidation states as more states become available in the 5d orbitals, but shielding dampens the effective nuclear charge so that transition energies are not noticeably affected by the oxidation state.[31, 32] The Ir-pyalk WOC sample in question having very similar XANES to that of IrO_2 suggested the catalyst to rest in the Ir^{IV} oxidation state, consistent with its characteristic blue color and previous XPS analysis.[24]

Analysis of the extended X-ray absorption fine structure (EXAFS) however revealed distinct differences in their respective structures. Figure 2 shows an overlay of the FT-EXAFS spectra of the IrO_2 reference and the Ir-pyalk WOC sample, revealing a similar first coordination shell (blue shaded section) but major differences in the longer-range order between the two samples (green shaded section).

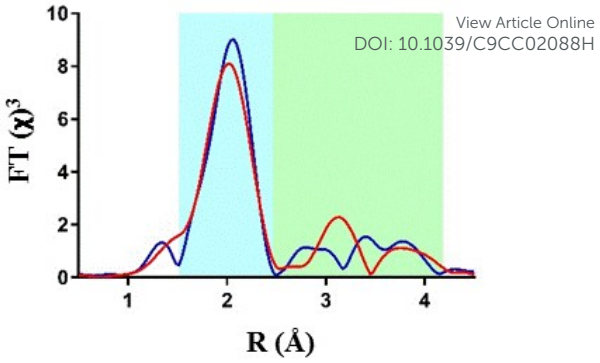

Figure 2. Comparison of Ir L_3 edge EXAFS data with k^3-weighting, showing Fourier transform EXAFS data for IrO_2 (red) and the Ir-pyalk WOC (blue).

The best fit parameters for the IrO_2 EXAFS spectrum showed the first coordinating shell around 2 Å to consist of six bridging oxygen atoms with a uniform Ir-O bond distance of 1.98 Å (Table 1). The similarity of the first shell between IrO_2 and Ir-pyalk WOC suggests a similar direct bonding environment to be present in the Ir-pyalk WOC sample (i.e. six low Z atoms around 2 Å). The analysis of peaks >2.5 Å of the IrO_2 spectrum required defining each single scattering contribution from the overlapping multiple backscattering pathways. These multiple scattering pathways are particularly prevalent in rigid, ordered structures such as crystalline metal oxides, but are known to be difficult to resolve for iridium due the absence of characteristic high amplitude peaks around 3 Å in the Fourier transform.[33] A comprehensive fitting analysis yielded optimum parameters indicating two neighboring Ir atoms at 3.11 Å and eight Ir atoms at 3.52 Å (Table 1, Table S1 and Figure S2), fully consistent with XRD results.[34]

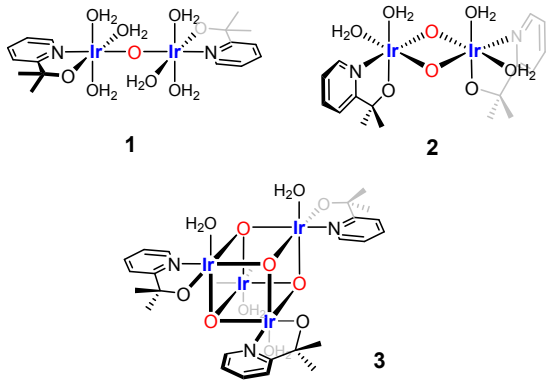

Figure 3. Three structural motifs used in the EXAFS fitting analysis of the Ir-pyalk WOC derived from [Cp*Ir(dimethyl-pyridinealkoxide)Cl] in dilute aqueous solution.

To fit the FT EXAFS spectrum of the Ir-pyalk WOC three structural motifs were investigated: a flexible mono-μ-oxo dimer (**1**)[25], a more rigid bis-μ-oxo dimer (**2**)[24], and a more extended "dimer of dimers" bis-μ-oxo cubane (**3**) (Figure 3, Table 1).

View Article Online
DOI: 10.1039/C9CC02088H

Table 1. Best parameters obtained from fitting the Ir L_3 edge EXAFS spectra of IrO_2 and Ir-pyalk WOC using structures **1-3** (brackets indicate a variable in the fitting; further details on the analysis including plots of all path contributions are given in Tables S1-3). Literature values for **1**[25] were used to fit the structure to our experimental data, where the path lengths and σ^2 values were fixed to the published distances.

Structure	Path	Distance (Å)	σ^2 (Å^2)	R_{fac}
IrO_2	6 Ir-O 2 Ir-Ir 8 Ir-Ir	1.98(1) 3.11(3) 3.52(8)	0.006(1) 0.006(3) 0.017(11)	0.001
1	6 Ir-O/N 2 Ir-C 4 Ir-C 1 Ir-Ir	2.04 2.81 2.97 3.56	0.004 0.009 0.006 0.002	0.014
2	2 Ir-O 4 Ir-O/N 1 Ir-Ir	1.96(1) 2.50(7) 2.97(4)	0.002 0.012(13) 0.002(3)	0.006
3	3 Ir-O 3 Ir-O/N 3 Ir-Ir	1.96(3) 2.04(3) 2.97(3)	0.006(4) 0.001(1) 0.012(3)	0.001

The bis-μ-oxo dimer structure **2** gave a high statistical fit for a short Ir-Ir distance of 2.97 Å with two bridging oxygen atoms, distinctly shorter than the 3.11 Å found in the "diamond core" of IrO_2 by XAS (Table 1) and XRD.[34] This contraction mainly originated from coordination of the chelating pyalk ligand, and not from a switch to μ^2-O from μ^3-O in IrO_2 (see also discussion of **3** below). With the four terminal N/O ligands from the pyalk ligand and coordinated water molecules forming the second shell, a good statistical fit with an R_{fac} (measure of fit accuracy, see SI) of 0.006 was obtained for **2** (Figure 4, Table S2). All attempts to fit the flexible mono-μ-oxo dimer **1**[25] to our EXAFS data yielded much poorer statistical fits of R_{fac} = 0.014 or higher. This arises due to the inclusion of a substantially increased Ir-Ir distance of 3.56 Å originating from the mono-μ-oxo unit. We found this to be incompatible with our EXAFS data showing that the Ir-Ir distance must be less than 3 Å, which cannot be obtained with a single oxo bridge between the metals.[35]

On the other hand, the even more rigid cubane structure **3** with three Ir contributions maintained the same Ir-Ir distance as found in **2**, with the remaining three N/O ligands moving to a shorter distance of 2.06(2) Å (Table S3, Figure 4). This arrangement provided an even better fit with a global R_{fac} of 0.001, showing excellent agreement with the EXAFS data out to *k* ranges beyond 10 Å^{-1} (Figure 4).

Inspecting the individual pathway contributions in the best fit analysis between structure **3** and **2**, only in the cubane structure **3** did the higher Ir coordination number adequately fit the shoulder peak contribution at 3.0 Å in the imaginary part of the Fourier Transform (Figure S6). In the dimer model **2** the Ir-Ir shell cannot fully reproduce this peak, requiring a shift to higher distance for the ligands to compensate, thus degrading the overall fit (Figure S6). This is indication that a nuclearity greater than two is present in the majority of the sample, with the best fitting analysis suggesting a neighboring iridium number of three as in the cubane structure **3**. Indeed, setting the Ir-Ir coordination number as a floating variable, the fitting optimization converged to an average of 2.6(4) neighboring Ir atoms. In addition, literature XRD data[36] are in good agreement with the Ir^{IV}-N/O distances of 2.05 Å as found in **3**.

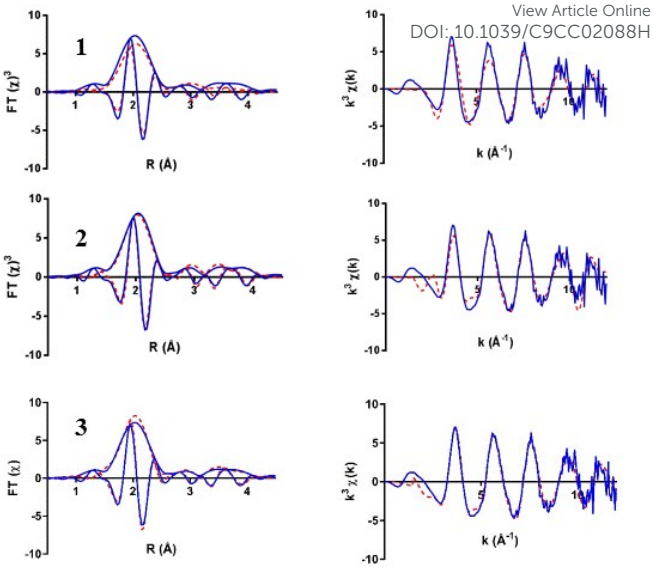

Figure 4. Ir L_3 edge EXAFS spectra of the Ir-pyalk WOC in solution (blue) comparing three simulated fit models from Figure 3 (red dashed): mono-μ^2-oxo dimer **1**, bis-μ^2-oxo dimer **2**, and bis-μ^3-oxo cubane **3**. Displaying k^3 weighted Fourier Transform (with imaginary part, left) and k^3 weighted EXAFS plot (right) for each structure.

Comparing structures **2** and **3**, the cubane differs in the reduction of terminal ligand sites from four to three, a shortening of Ir-N/O distances from 2.51 Å to 2.04 Å, and an increase of neighboring Ir atoms from one to three in the tetranuclear oxo-cubane. This provided a superior statistical fit with realistic bond distances for structure **3** even compared to the good fit for structure **2**. This analysis shows both bis-μ-oxo dimers and tetramers to be viable possibilities, with the EXAFS fit indicating an oxo-cubane type 'dimer-of-dimer' structure **3** to be the most realistic structural representation of the resting state of the activated Ir-pyalk WOC in aqueous solution.

We have provided a detailed structural analysis of a prominent molecular WOC through iridium L_3 edge XAS. The results find mono-μ-oxo linkages to allow too much flexibility and induce too large Ir-Ir distances to be compatible with experimental EXAFS data of the resting state of the activated catalyst, suggesting that such species may not be relevant to water oxidation catalysis.[35] Our analysis points to more compact and rigid bis-μ-oxo linkages in oxo-cubane 'dimer-of-dimers' as the key structural feature in these highly active and durable WOCs. Similar metal-oxo cubanes have been shown to feature in a number of WOCs based on other transition metals such as Mn, Co, and Ni (including the natural OEC in PSII),[27, 37] and their unique robustness and redox chemistry may represent a common design criterion allowing for high activity and stability in the demanding 4-electron oxidation of water. Importantly, a pyalk-modified bis-μ-oxo Ir_4O_4 cubane would be consistent with previously reported characterization data including ^{17}O NMR, EPR, UV-vis and resonance-Raman spectroscopies,[24] and shed new light on the mode of surface binding of these catalysts.[38, 39] However, we caution that the kinetic role of such tetrameric

resting states will have to be clarified prior to mechanistic interpretations. Recently a half order in [Ir] on the rate of O_2 evolution has been found for a range of pyalk-ligated Ir WOCs using $NaIO_4$, implying a dominant dimeric resting state liberating small amounts of active monomer into the catalytic cycle.[40] In light of the present findings this could mean a tetramer-dimer, or tetramer-dimer-monomer equilibria to be operational instead. Ascertaining how many metal sites are involved in the turnover-limiting step will be important for deciphering the workings of these highly active catalysts.

Conflicts of interest

U.S. Patent 9/790/605 by SWS, UH *et al.* contains intellectual property described in this article. The other authors declare no competing financial interest.

Acknowledgements

This work was supported by the Royal Society (UF160458; University Research Fellowship to UH), the EPSRC Centre for Doctoral Training in Sustainable Chemical Technologies (EP/L016354/1; PhD studentship to EVS), and the UK Catalysis Hub (EP/K014714/1). The authors would like to thank Mark Styles and Nathan Webster (CSIRO, Australia), Robert Potter (Johnson Matthey), and Paul Frith (University of Bath) for their support and assistance with this project.

Notes and references

1. Nicola, A.; Vincenzo, B., *Angewandte Chemie International Edition* 2007, **46** (1-2), 52.
2. Ioannis, K.; Serhiy, C.; R., Z. A.; J., M. K. J., *Angewandte Chemie International Edition* 2014, **53** (1), 102.
3. Kärkäs, M. D.; Verho, O.; Johnston, E. V.; Åkermark, B., *Chemical Reviews* 2014, **114** (24), 11863.
4. Blakemore, J. D.; Crabtree, R. H.; Brudvig, G. W., *Chemical Reviews* 2015, **115** (23), 12974.
5. McCrory, C. C. L.; Jung, S.; Peters, J. C.; Jaramillo, T. F., *Journal of the American Chemical Society* 2013, **135** (45), 16977.
6. Steegstra, P.; Busch, M.; Panas, I.; Ahlberg, E., *The Journal of Physical Chemistry C* 2013, **117** (40), 20975.
7. Minguzzi, A.; Locatelli, C.; Lugaresi, O.; Achilli, E.; Cappelletti, G.; Scavini, M.; Coduri, M.; Masala, P.; Sacchi, B.; Vertova, A.; Ghigna, P.; Rondinini, S., *ACS Catalysis* 2015, **5** (9), 5104.
8. Minguzzi, A.; Lugaresi, O.; Achilli, E.; Locatelli, C.; Vertova, A.; Ghigna, P.; Rondinini, S., *Chemical Science* 2014, **5** (9), 3591.
9. G., S. C. H.; Ling, N. M.; Sarp, K.; Daniel, F.; Hirohito, O.; Anders, N., *Angewandte Chemie International Edition* 2014, **53** (28), 7169.
10. Pfeifer, V.; Jones, T. E.; Wrabetz, S.; Massué, C.; Velasco Vélez, J. J.; Arrigo, R.; Scherzer, M.; Piccinin, S.; Hävecker, M.; Knop-Gericke, A.; Schlögl, R., *Chemical Science* 2016, **7** (11), 6791.
11. Ooka, H.; Wang, Y.; Yamaguchi, A.; Hatakeyama, M.; Nakamura, S.; Hashimoto, K.; Nakamura, R., *Physical Chemistry Chemical Physics* 2016, **18** (22), 15199.
12. Bergmann, A.; Zaharieva, I.; Dau, H.; Strasser, P., *Energy & Environmental Science* 2013, **6** (9), 2745.
13. Over, H., *Chemical Reviews* 2012, **112** (6), 3356.
14. Risch, M.; Khare, V.; Zaharieva, I.; Gerencser, L.; Chernev, P.; Dau, H., *Journal of the American Chemical Society* 2009, **131** (20), 6936.
15. McEvoy, J.; Brudvig, G. W., *Chemical Reviews* 2006, **106** (11), 4455.
16. Thomsen, J. M.; Huang, D. L.; Crabtree, R. H.; Brudvig, G. W., *Dalton Transactions* 2015, **44** (28), 12452.
17. Artero, V.; Fontecave, M., *Chemical Society Reviews* 2013, **42** (6), 2338.
18. Michaelos, T. K.; Shopov, D. Y.; Sinha, S. B.; Sharninghausen, L. S.; Fisher, K. J.; Lant, H. M. C.; Crabtree, R. H.; Brudvig, G. W., *Accounts of Chemical Research* 2017, **50** (4), 952.
19. Hintermair, U.; Hashmi, S. M.; Elimelech, M.; Crabtree, R. H., *Journal of the American Chemical Society* 2012, **134** (23), 9785.
20. Thomsen, J. M.; Sheehan, S. W.; Hashmi, S. M.; Campos, J.; Hintermair, U.; Crabtree, R. H.; Brudvig, G. W., *Journal of the American Chemical Society* 2014, **136** (39), 13826.
21. Sheehan, S. W.; Thomsen, J.; Hintermair, U.; Crabtree, R. H.; Brudvig, G. W.; Schmuttenmaer, C. A., *Nature Communications* 2015, **6**, 6469.
22. Li, W.; Sheehan, S. W.; He, D.; He, Y.; Yao, X.; Grimm, R. L.; Brudvig, G. W.; Wang, D., *Angewandte Chemie International Edition* 2015, **54**, 11428.
23. Moir, J. W.; Sackville, E. V.; Hintermair, U.; Ozin, G. A., *The Journal of Physical Chemistry C.* 2016, **120** (24) 12999.
24. Hintermair, U.; Sheehan, S. W.; Parent, A. R.; Ess, D. H.; Richens, D. T.; Vaccaro, P. H.; Brudvig, G. W.; Crabtree, R. H., *Journal of the American Chemical Society* 2013, **135** (29), 10837.
25. Yang, K. R.; Matula, A. J.; Kwon, G.; Hong, J.; Sheehan, S. W.; Thomsen, J. M.; Brudvig, G. W.; Crabtree, R. H.; Tiede, D. M.; Chen, L. X.; Batista, V. S., *Journal of the American Chemical Society* 2016, **138** (17), 5511.
26. Sharninghausen, L. S.; Sinha, S. B.; Shopov, D. Y.; Choi, B.; Mercado, B. Q.; Roy, X.; Balcells, D.; Brudvig, G. W.; Crabtree, R. H., *Journal of the American Chemical Society* 2016, **138** (49), 15917.
27. Yano, J.; Kern, J.; Sauer, K.; Latimer, M. J.; Pushkar, Y.; Biesiadka, J.; Loll, B.; Saenger, W.; Messinger, J.; Zouni, A.; Yachandra, V. K., *Science* 2006, **314** (5800), 821.
28. Li, X.; Clatworthy, E. B.; Bartlett, S. A.; Masters, A. F.; Maschmeyer, T., *The Journal of Physical Chemistry C* 2017, **121** (21), 11021.
29. Lebedev, D.; Pineda-Galvan, Y.; Tokimaru, Y.; Fedorov, A.; Kaeffer, N.; Copéret, C.; Pushkar, Y., *Journal of the American Chemical Society* 2018, **140** (1), 451.
30. Sackville, E. V.; Kociok-Köhn, G.; Hintermair, U., *Organometallics* 2017, **36** (18), 3578.
31. Uzan, A.; Gates, B. C., *Angewandte Chemie International Edition* 2008, **47** (48), 9245.
32. Choy, J. H.; Dong-Kuk, K.; Demazeau, G.; Jung, D. Y., *The Journal of Physical Chemistry* 1994, **98**, 6258.
33. Prouzet, E., *Journal of Physics: Condensed Matter* 1995, **7**, 8027.
34. Bolzan, A. A.; Fong, C.; Kennedy, B. J.; Howard, C. J., *Acta Crystallographica Section B* 1997, **B(53)**, 373.
35. *A possible explanation for previous findings of Ir-Ir distances of ~3.5 Å, leading to the proposal of mono-μ-oxo structures, could be the fact samples had been prepared at much higher Ir concentrations in advance of the analysis. This may have led to the formation of IrO_2 particles that give Ir-Ir backscattering peaks in exactly that region (see Table 1), which we did not observe in homogeneous samples freshly prepared below the critical Ir concentration of 10 mM.*
36. Sinha, S. B.; Shopov, D. Y.; Sharninghausen L. S; Stein, C. J.; Mercado, B. Q.; Balcells, D.; Pedersen, T.; Reiher, M.; Brudvig, G.W.; Crabtree, R. H., *Journal of the American Chemical Society* 2017, **139**, 9672.
37. Song, F.; Moré, R.; Schilling, M.; Smolentsev, G.; Azzaroli, N.; Fox, T.; Luber, S.; Patzke, G. R., *Journal of the American Chemical Society* 2017, **139** (40), 14198.
38. Zhao, Y; Yang, K. R.; Wang, Z.; Yan, X.; Cao, S.; Ye, Y.; Dong, Q.; Zhang, X.; Thorne, J. E.; Jin, L.; Materna, K. L.; Trimpalis, A.; Bai, H.; Fakra, S. C.; Zhong, X.; Wang, P.; Pan, X.; Guo, J.; Flytzani-Stephanopoulos, M.; Brudvig, G. W.; Batista, V. S.; Wang, D., *PNAS* 2018, **115** (12) 2902.
39. Zhao, Y; Yan, X.; Yang, K. R.; Cao, S.; Dong, Q.; Thorne, J. E.; Materna, K. L.; Zhu, S.; Pan, X.; Flytzani-Stephanopoulos, M.; Brudvig, G. W.; Batista, V. S.; Wang, D., E, *ACS Central Science* 2018, **4** (9) 1166.
40. Sackville, E. V.; Marken, F.; Hintermair, U., *ChemCatChem* 2018, **10** (19), 4280.